Observations and Process Parameter Sensitivities in Fluid-Bed Granulation

S. A. Cryer and P. N. Scherer
Dow AgroSciences, 9330 Zionsville Rd., Indianapolis, IN 46268

A numerical approach using mechanistic modeling (population balance) for fluid-bed agglomeration is documented elsewhere. Here important factors for a pilot-scale fluid-bed granulater as determined by a 1/2 fraction factorial statistical design of experiment (DOE), Monte Carlo analysis of the mechanistic model, and comparison of experimental observations to model predictions, are summarized. DOE results indicate sensitive primary process parameters affecting granule size include the bed bowl charge, binder spray rate, air flow rate, and input air temperature. Sensitivity analysis of model results suggest the binder spray rate accounts for approximately 65% of the predicted variance, with the next most sensitive parameter the binder droplet diameter (~11%). Population balance modeling specifically for fluid beds, coupled with a DOE can be combined so the behavior of agglomeration of wettable powders within a fluid bed can be understood and predicted. Good agreement between experiment and simulation results is found for particles grown to sizes of industrial importance.

Introduction

Granules and agglomeration

Wet granulation is the process of converting small-diameter solid particles (typically powders) into larger-diameter agglomerates made up of the initial particles. A liquid binder solution (or water) is sprayed onto the powder to form a thin layer of liquid surrounding a particle. Liquid pendular bridges are formed as wetted particles coalesce and subsequently form a nonfriable structure once the water is evaporated off. The resulting stable agglomerate particle is therefore "grown" from a smaller size into a larger agglomerate particle, as measured by a mean particle volume or diameter.

Fluid-bed agglomeraters were introduced into the United States by the pharmaceutical industry in 1975 as a means to prepare granulated material (Olsen et al., 1985). An advantage of using a fluid bed is that many steps can be performed in the same piece of equipment. These steps include preblending of the powder (if appropriate), granulation with a suitable liquid binding agent, followed by drying of the granules to a predetermined moisture content. Figure 1 represents a typical fluid-bed granulater operating in batch mode. Powder is initially charged into the fluid-bed system. Air is then forced into the granulater at the bottom of the column. A mesh/screen keeps powder from leaving at the bottom, while filters at the top of the column allow air to pass, but keep solid particles from leaving. These filters are periodically shaken to dislodge any particles to return them back to the fluid bed. Once the powder is fluidized (and mixed if appropriate), a binder agent consisting of water with 5% polyvinylpyrrolidone (PVP—a water-soluble synthetic protein like substance) is pumped and subsequently atomized into fine droplets before being added to the fluid bed. The addition of the binder begins the nucleation/agglomeration process. Once the granules are grown to an appropriate size, the binder-solution flow rate is terminated and the granules are then allowed to dry during the drying regime as air is continually being passed through the system.

An experimental program was initiated to investigate the role and sensitivity of process variables on output attributes of interest. This work focuses on granule size and growth kinetics, although other attributes such as porosity or attrition strength could be examined as well, if these attributes are known or measured. Results from the experimental program are used to statistically determine important process vari-

Correspondence concerning this article should be addressed to S. A. Cryer.

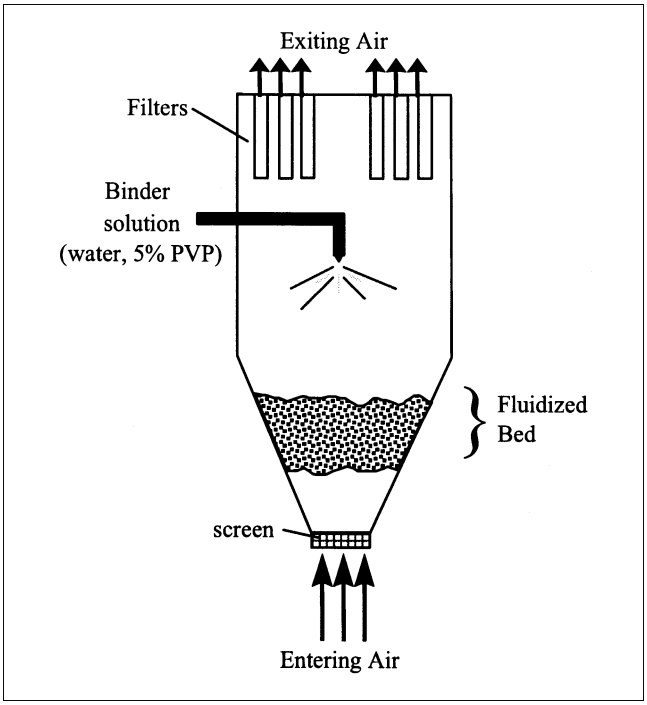

Figure 1. A typical fluid-bed granulater.

ables and in model validation for a proposed fluid-bed model (Cryer, 1999) based upon population balance methodologies.

Examples of design of experiments (DOE) for fluid-bed granulation can be found elsewhere (Kao et al., 1996; Aulton and Banks, 1978). The work of Aulton and Banks is limited to empirical interpretation of granule endpoint as "good" or "poor" based upon flow and tabletability (tablet characteristics such as compaction and crushing strength) of the ending granule. Kao et al. used a two-way factorial design to examine the effects of air volume, inlet air temperature, nozzle size, spraying air pressure, and spraying rate, on the formation of lactose granules in a fluidized-bed granulater, as related to the granule geometric mean diameter at the experimental run conclusion. All primary factors were found to significantly affect granule size. In addition, a two-factor ANOVA regression model was found to fit the experimental data quite well ($R^2 = 0.94$), suggesting causal effect between process variables and granule properties do exist in fluid-bed granulation. Air volume, inlet air temperature, and spray rate of binder are all factors used in the current DOE presented here.

Materials and Methods

Experimental

The experimental apparatus was a commercial Glatt GPCG 5/30 operated in batch mode, having a conical shaped 120-L bowl that was used for the 30-kg batches in this study. Samples of powder/granules from the fluid bed are taken at equally spaced intervals of 1 kg of binder solution added (that is, intervals of 0, 1, 2, …, n (kg) of cumulative binder added). Binder addition was chosen as a consistent temporal unit of measure, since the binder flow rate was altered in a discrete, 3-step process for the experimental trials. If the binder flow was too fast, the agglomeration process was rapid and difficult to control, as granules grew in an exponential fashion. The weight and drag associated with sufficiently large granules was beyond the ability of the fluid bed fan to keep the bed fluidized, and loss of fluidization would ensue. Rapid growth rates were often observed near the end of an experimental run. Thus, binder flow rate was decreased over time to yield a controllable agglomeration process near the experiment terminus. Since the binder spray rate changes throughout an experimental trial, a unit of 1 kg of spray does not necessarily correspond to an equal time interval between samples. Granule/powder particle size distributions are measured off-line using a Sympatec Helos laser defraction instrument that incorporated an automatic feed mechanism. Particle distributions from 0.1 μm to 1,000 μm could be quanti-

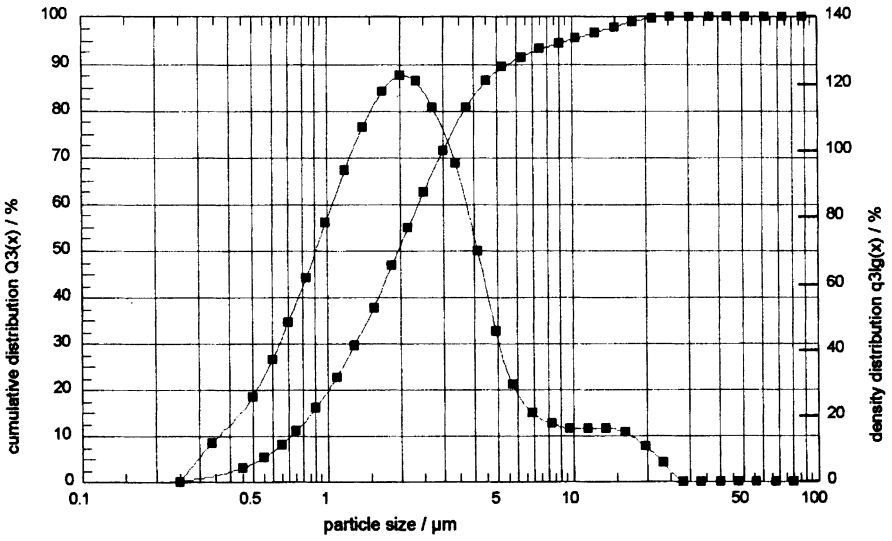

Figure 2. Starting particle-size distribution (powder) given as a discrete density and cumulative distribution.

Table 1. Description of the Fluid-Bed Process Parameters

Parameter	Description
Temperature	Temperature of entering air to fluidize the bed (40–60°C)
Air Flow	Volumetric flow rate of fluidizing air ($0.106–0.153\ m^3 \cdot s^{-1}$)
Binder Spray Rate	Spray rate of liquid binder solution ($222–325\ g \cdot min^{-1}$ ($3.70 \times 10^3 – 5.42 \times 10^3\ kg \cdot s^{-1}$)}
Bowl Charge	Mass of power initially charged into the batch-operated fluid bed (25–35 kg)
Nozzle Height	Nozzle height position of spray nozzle for binder within the fluid bed (Positions 1, 3)

fied, although a span of this magnitude entailed an instrument lens change on the Sympatec unit.

Flumetsulam, a commercial Dow AgroSciences product, was the starting material used (specific gravity 1.57, water solubility 123 mg/L). This material was the same as that used in manufacturing, in terms of the milling process to create the starting powder. The particle-size distribution (PSD) for the starting powder represented as both a probability density function and cumulative distribution can be seen in Figure 2. The volume median diameter for this powder is approximately 2.0 μm, which classifies the powder in the submicron range.

Process sensitivity analysis and design of experiments

A statistical DOE was constructed to identify important factors regarding granulation in the Glatt fluid bed. A 1/2 fractional factorial DOE with five factors was employed to keep the number of experimental runs to a minimum. Controlled factors are: temperature (40°C, 60°C), air flow (low, high), binder spray rate (low, high), bowl charge (25 kg, 35 kg), and nozzle height (1,3). Input parameter ranges were based upon earlier trial-and-error experiments that attempted to map out the input parameter response-surface. Parameter ranges were based upon prior observations regarding granule kinetic growth to sizes of industrial importance over the time scale of a commercial run. Descriptions for these parameters are summarized in Table 1.

Combinations of the high and low levels of the five factors yielded 16 runs that were performed in random order. Each experimental trial takes between 2 and 3 hours (not including sample analysis or cleaning of the equipment). The design of experiments with parameter magnitudes can be seen in Table 2.

The final sample taken at the end of each experimental trial was analyzed for particle size to characterize the ending-size distribution. This quantification captured X10 (the granule size capturing the smallest 10% of the sample), X16, X50, X84, X90, X99, and the volume median diameter (VMD) for the transient granule size distribution. Any of these measurements can be used in the sensitivity analysis as endpoints to characterize how the experimental factors influence the resulting granule-size distribution. However, the statistical analysis is restricted to the VMD endpoint when tracking the kinetic growth of the granules.

MINITAB Release 12.2 and S-Plus Version 4.5 statistical software packages were used for all statistical graphs and analyses. The experimental design was analyzed using standard linear models that allow investigation of the significance of the design factors and any two-way interactions. The main effects and interaction plots are used to display the respective effects. Higher level (than two-way) interaction effects cannot be explored with a 1/2 fractional factorial design.

Table 2. $\frac{1}{2}$ Fraction Factorial DOE

Run Order	Temp.	Air Flow	Spray Rate	Bowl Charge	Nozzle Height
1	40	Low	Low	35	1
2	60	Low	High	35	1
3	60	High	High	35	3
4	60	High	Low	35	1
5	40	Low	Low	25	3
6	40	Low	High	25	1
7	60	High	Low	25	3
8	40	High	High	35	1
9	60	High	High	25	1
10	40	Low	High	35	3
11	60	Low	Low	25	1
12	40	High	High	25	3
13	40	High	Low	35	3
14	40	High	Low	25	1
15	60	Low	Low	35	3
16	60	Low	High	25	3

Numerical model

Ennis et al. (1990) proposed that strength of the dynamic bridge formed between colliding particles surrounded by a binder fluid is an order of magnitude greater than the static force governed by the Laplace-Young equation. Thus, the strength of the dynamic liquid bridge governs the rate of granule consolidation while providing an explanation of the mechanism for coalescence. Coalescence will occur for colliding granules having insufficient relative kinetic energy to overcome the viscous dissipation force due to the surrounding binder fluid. Ennis and coworkers postulated that the transition for agglomeration/rebound of colliding particles is parameterized by a critical Stokes number (S_t^*), where the definition for the Stokes number (S_t) is

$$S_t = \frac{4\rho U_c d}{9\mu} \tag{1}$$

where ρ-is granule density, U_c is relative collisional velocity, d is average granule diameter, and μ is solution phase binder viscosity.

The binder solution viscosity (μ) and the granule density are largely properties of the feed and binder solution. The collisional velocity is a function of both the type of granulation equipment and process variables that affect bed agitation. The Stokes number represents a measure of inertia (initial collisional kinetic energy) to viscous effects occurring during agglomeration.

Details of a discretized population balance (DPB) model for fluid bed agglomeration are found elsewhere (Cryer, 1999). The Stokes number was linked to important process variables (air and binder flow rate, bed charge, bed geometry). Thus, the physical processes governing particle coales-

cence and rebound within a fluid bed are functions of process variables and coefficients parameterizing coalescence (kernel). The coalescence kernel governs the rate and extent for agglomeration (or particle rebound) as two particles come together and collide. Using the Stokes number to define agglomeration has been proposed by other researchers to define coalescence kernel coefficient magnitudes (Adetayo and Ennis, 1997; Ennis et al., 1991). Cryer (1999) proposed a new coalescence kernel (Eqs 2–3) based upon physical insight, simplicity, and deterministic equivalent modeling (Tatang, 1995) to account for uncertainty. This kernel is based upon a Stokes number methodology where uncertainty in the Stokes number is characterized by polynomial chaos expansions. The coalescence kernel coefficient (β) is represented as

$$\beta = \beta_o \int_{-\infty}^{S_{t^*}} f(\phi,t)\, d\phi \tag{2}$$

where $f(\phi,t)$ is discrete probability density function for the Stokes number, β_o is constant determined from experimental data and S_t^* is critical Stokes number.

Advantages of the proposed kernel include (1) simplicity, (2) physically based on Stokes number methodology, (3) is easily incorporated into a numerical modeling procedure, (4) accounts for uncertainty in parameter predictions/calculations, (5) can model similar behavior of other proposed kernels with fewer "free parameters," and (6) can be used to explain the noninertial granule growth regimes often seen experimentally. S_t^* is treated as a free parameter that Cryer assumed to be characterized by Eq. 3. Equation 3 illustrates a function where S_t^* increases with time, and the percentage of collisions resulting in coalescence can also increase. Depending upon the sign and magnitude of α_2, S_t^* can either increase or decrease with time. If α_2 is greater than the time scale of the experiment, then S_t^* remains constant for all time

$$S_t^* = \alpha_1(1 + e^{t-\alpha_2}) \tag{3}$$

Three free parameters are required to fully characterize the coalescence kernel behavior over the fluid-bed response surface (Eq. 2), as proposed by Cryer. These coefficients, α_1, α_2 (for determining S_t^*), and β_o, can be estimated through comparison between model predictions and experimental observations.

Results and Discussion

DOE analysis

Observations for process variable sensitivity are consistent with the physics on which the model is based. The kinetic energy associated with two colliding particles must first be dissipated before agglomeration can occur. The ability to dissipate the inertia of two colliding particles increases as the powder/granules are coated with a liquid layer (binder). As the number of particles being wetted increases or as the liquid layer surrounding a particle increases, the coalescence rate (and, thus, VMD) will increase due to the viscous dissipation capability of the binder layer around a particle. A low bowl charge increases the binder layer around a single particle as there are fewer particles to be wetted for the same binder spray rate. Similarly, increases in binder spray rate increase the amount of binder present in the system for wetting particles (and thus the ability of two wet particles/granules to agglomerate). Air flow and temperature should effect VMD, since air properties provide a mechanism for drying any binder (liquid) layer surrounding a particle. Therefore, as the air flow increases, VMD should decrease. As the air temperature decreases, the water saturation limit of the air also decreases. Thus, the air is "dryer" at the lower temperatures. This dryer air creates a mass-transfer driving force between any water in the granulater with the air flowing through. Thus, as the humidity in the air is decreased (decreasing air temperature), evaporation increases, and, thus, the binder layer surrounding a particle decreases. This creates an environment for increased particle rebound (that is, coalescence decreases), and, thus, VMDs are lower.

Table 3. ANOVA Table for the Fractional Factorial DOE

Term	Coef.	T	P Value (P)
Constant	98.16	72.69	0
Temperature	13.25	9.81	0.001
Air flow	13.73	10.16	0.001
Spray rate	−27.51	−20.37	0
Bowl charge	−19.5	−14.44	0
Nozzle height	3.17	2.35	0.078
Temperature* spray rate	−17.58	−13.01	0
Temperature* bowl charge	−9.16	−6.78	0.002
Temperature* nozzle height	−9.94	−7.36	0.002
Air flow* bowl charge	4.39	3.25	0.031
Spray rate* bowl charge	−11.67	−8.64	0.001
Spray rate * nozzle height	−16.65	−12.33	0

Analysis of Variance (ANOVA). Table 3 summarizes ANOVA results for modeling VMD on the five design factors and their interactions. The parameter "Coef" in Table 3 stands for the linear regression equation coefficients. In this table T and P represent the "T-statistic" assuming a "T" distribution, while P represents the level of significance or P-value (P). Sensitive process parameters are taken to be those whose P value is small ($P \leq 0.01$). Spray rate and bowl charge have the largest effect ($P = 0$), whereas nozzle height appears to have little impact on the resulting VMDs ($P = 0.078$). The sign ($\pm$) of the effect coefficient determines the behavior of granulation on this parameter. A positive sign suggests that increases in that parameter will result in increases in granule size, while the converse is true for effect parameters having a negative sign. Thus, entering air temperature, spray rate, and nozzle height (low) are associated with higher VMDs. Increases in entering air flow and bowl charge are associated with lower VMDs.

Five of the ten possible two-way interactions are of statistical significance. Several borderline interactions are also included in Table 3. Although the "air flow * bowl charge" interaction is found to be of borderline significance, it is a comparatively small effect and perhaps worthy of only modest consideration. Conclusions drawn from the ANOVA table are that the two-way interactions of temperature and spray rate interact vigorously with all factors except for air flow. Interactions involving bowl charge and nozzle height appear to be somewhat less general, though still of importance, and air temperature and flow, binder spray rate, and bowl charge

are all primary process variables having a strong influence on granule VMD.

Higher than two-way interactions could not be investigated using the 1/2 fraction DOE. However, higher than two-way interactions can be qualitatively addressed by viewing the interaction plot (Figure 3). Sharp differences in the slope between "low"(dashed) and "high"(solid) parameter values are indicative of sensitive two-way interactions, as is borne out by the ANOVA and represented graphically in Figure 3. Lines with nearly identical slopes are indicative of negligible interactions (that is, $P > 0.01$). Notice that the effect of nozzle height is very different for temperature and spray rate. Little temperature difference is noted at the high nozzle height, but at this same nozzle height a dramatic effect due to spray rate is observed. A reciprocal pattern is observed at the low nozzle height. This would strongly suggest a three-way interaction between temperature, spray rate, and nozzle height does exist. No other clear indicators of three-way interactions are qualitatively observed, though it is quite possible that other interactions can and do exist.

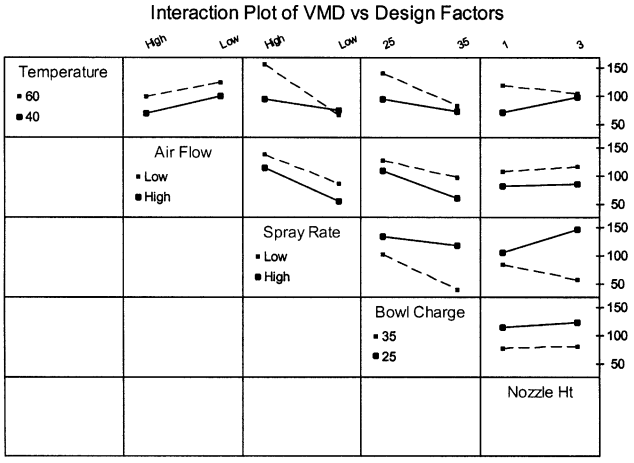

Figure 3. Interaction plot for two-way interactions for process variables (design factors).

Model evaluation

The numerical model developed by Cryer (1999) can be used with the DOE trials to incorporate the continuous and discrete aspects associated with the binder flow rate (and other process variables). Instead of statistically inferring which process variables are important, we focus on quantifying model parameters using the observations of the DOE trials. Unknown parameters in the model deal with the rate and extent of granulation, as given by the coalescence kernel parameters (α_1, α_2, β_o). Coalescence kernel coefficients are determined for each DOE trial based upon a modified flexible-polygon search procedure (Himmelblau, 1972) in minimizing the sum of squared residuals between model predictions and experimental observations. Actual process variables for each trial are used in the modeling process.

Relating Process Variables to Granule Size. Table 4 summarizes the findings for the coalescence kernel coefficients for each DOE experimental trial (plus four other center-point runs), as predicted by the optimization program coupled with the DPB model. A center point is defined as the point midway between a high and low input parameter. The magnitude of the coefficients found in Table 4 should be identical if the coalescence kernel given by Eqs. 2 and 3 adequately represents the physics occurring in the agglomeration process. This is not observed, which indicates that a more complex kernel is required to capture the agglomeration behavior seen experimentally. This is not to say the kernel given by Eqs. 1, 2 and 3 cannot capture experimental behavior, but rather that the coefficients found in this kernel are not constants but, in fact, functions of other properties or parameters. Thus, an empirical approach is used to estimate the correlation between the coalescence kernel coefficients (α_1, α_2, β_0) and process variables (since the process variables for each experimental trial are known).

Regression Analysis. Results of the DOE analysis indicate that two-way (and possibly higher) interactions are important

Table 4. Coalescence Kernel Coefficients

Exp. No.	Objective Function	α_1 (dimensionless)	α_2 (s)	β_0 (dimensionless)
0	3.88*E*-03	1050	2462.1	$1.19E+03$
1	$6.22E-03$	803	2897.2	$2.36E+03$
2	$6.69E-03$	2700	2354.3	$2.15E+03$
3	$2.37E-03$	748	1936.8	$3.44E+03$
4	$2.97E-01$	1440	2090.4	$1.53E+04$
5	$2.40E-03$	589	3626.9	$1.51E+02$
6	$1.51E-02$	3490	4378.6	$6.31E+02$
7	$5.34E-02$	1540	5286.4	$5.76E+02$
8	$1.19E-03$	275	1309.4	$2.31E+02$
9	$1.62E-02$	395	2118.5	$4.18E+03$
10	$1.36E-02$	358	2412.3	$2.24E+03$
11	$7.38E-03$	1220	348.2	$1.32E+03$
12	$5.21E-03$	2030	160.6	$9.12E+02$
13	$1.49E-02$	606	332.2	$3.18E+03$
14	$9.08E-02$	370	2931.1	$3.69E+04$
15	$1.09E-01$	518	1535.7	$1.32E+05$
16	$3.11E-02$	150	2186.2	$3.92E+03$
17	$5.09E-02$	728	2600.2	$3.05E+04$
18	$1.87E-02$	237	2240.3	$4.60E+03$
19	$2.16E-03$	35.6	2519.0	$8.34E+02$
20	$7.69E-02$	569	1389.8	$7.55E+04$

Table 5. R^2 Values for Linear Correlation of Process Variables and Coalescence Coefficients (Eqs. 3–4)

Parameters	2nd order	3rd order
α_1	0.63	0.67
α_2	0.78	0.88
β_o	0.71	0.95

with respect to the endpoint of VMD. Instead of qualitatively analyzing whether interactions of multiple process parameters are found to impact VMD, as is performed for the DOE, we explore the effect of using linear modeling to represent the coalescence kernel coefficients as functions of process variables. An integral average for a process variable (for use in the linear model procedure) was calculated over the time of the experiment when variables were time dependent.

Several linear regression models are proposed to describe kernel-parameter dependence on process variables. Both second- and third-order polynomials are used (Eqs. 4 and 5), where P_i represents the process variable (air temperature, binder spray rate, air flow rate, bowl charge). The coefficients $b_0, b_{i,j}, b_{i,j,k}$ are coefficients determined from the linear regression where independent variables (P_i) and dependent variables $\{Q_i = \ln(\alpha_1), \ln(\alpha_2), \beta_o\}$ have been provided to the fitting routine

$$Q_i = b_o + \sum_{i=1}^{n} b_i P_i + \sum_{i=1}^{n} \sum_{j=2}^{n} b_{i,j} P_i P_j (i \neq j) \quad (4)$$

$$Q_i = b_o + \sum_{i=1}^{n} b_i P_i + \sum_{i=1}^{n} \sum_{j=2}^{n} b_{i,j} P_i P_j (i \neq j) + \sum_{i=1}^{n} \sum_{j=2}^{n} \sum_{k=2}^{n} b_{i,j,k} P_i P_j P_k (i \neq j \neq k) \quad (5)$$

where

$$Q_i = \ln(\alpha_1), \ln(\alpha_2), \text{ or } \beta_0$$

Table 5 summarizes the regression results using Eqs. 4 and 5. Equation 5 (with appropriate predetermined coefficients) has been incorporated into the model proposed by Cryer for fluid-bed granulation. Thus, the model user need only supply process variables for a scenario of interest, and the model predicts the magnitudes for the coalescence kernel coefficients as given by Eq. 5 with known constants (that is, no need to solve the inverse problem). With the coalescence kernel coefficients known, the DPB modeling system can then be used to estimate transient granule growth and particle-size distributions of the final products for specific process and geometric constraints the user is interested in.

Implementation of regression analysis into DPB model

This "hybrid" mechanistic–empirical model was executed using the correlation analysis between the three-parameter coalescence kernel coefficients and process variables. The word "hybrid" is added, since the coalescence kernel coefficients are now empirically related to process variables. Figure 4 contains a representative comparison of the DPB model predictions to experimental observations for three distinct agglomeration experiments (slow, medium, and rapid agglomeration rates). The DPB model captures the correct magnitudes and trends for different experiments manifesting different agglomeration rates.

Figure 5 represents model results obtained by the hybrid model when the transient nature of the granule-size distribution is addressed. The DPB modeling system overestimates the lower end of the particle-size distribution early in the granulation process, indicating that a more complex coalescence kernel and/or mechanism is governing the coalescence process. However, modeling of the agglomeration process using a DPB with the proposed three-parameter Stokes-number kernel at later times (when the particle-size distribution is of industrial importance) is adequate to address optimiza-

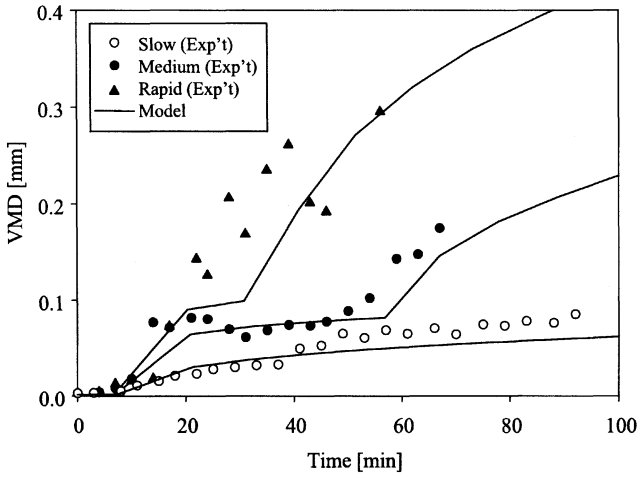

Figure 4. Experimental observations of granule size during agglomeration for three different growth-rate experiments vs. hybrid DPB model containing regression equations for coalescence kernel parameters.

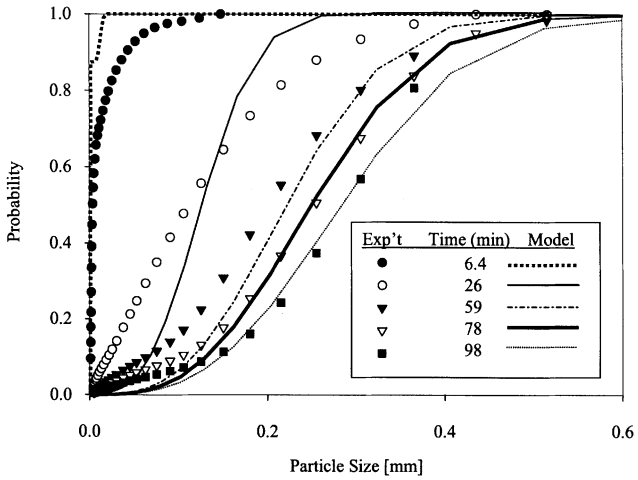

Figure 5. Experimental observations and model predictions of particle-size distribution for granule growth; DOE trial No. 9, 3-parameter coalescence kernel using regression for kernel coefficients.

Table 6. Input Properties for Monte Carlo Simulation and Sensitivity Analysis

Parameter	Description	Normal Distrib. (μ, σ), Unless Indicated
Temp − air − exit	Temperature of air leaving granulater (°C)	(23.0, 4.60)
Temp(i)i = 1,3	Temperature of entering fluidizing air (°C)for time $T(i)$	(60, 12); (60, 12); (60, 12)
T (i)i = 1,3	Time when $Q(i)$, temp (i), and dew (i) take effect (min)	(0, 0); uniform (25−35); uniform (35−45)
$T1$ (i)i = 1,3	Time when binder (i) takes effect (min)	(0, 0); uniform (25−35); uniform (35−45)
Q(3)i = 1,3	Volumetric flow rate of fluidizing air (cm^3/h)]	$(9.3\times10^8, 1.87\times10^8)$; $(2.09\times10^9, 2.16\times10^8)$; $(1.43\times10^9, 2.86\times10^8)$
Min powder dia.	Powder minimum dia.	$(6.21\times10^{-4}, 1.242\times10^{-4})$
Max powder dia.	Powder maximum dia.	$(2.00\times10^{-3}, 4.00\times10^{-4})$
Powder density	Bulk density of starting powder (g/cm^3)	(1.30, 0.26)
Nuc/agg trans	Transition from nucleation to agglomeration as measured by mass of binder addition (kg)	(3.00, 0.60)
NOR	No. of orifices per unit area of * distributor plate (cm^{-2})	(0.96, 0.19)
Moisture powder	Moisture content of powder (%) at experiment onset	(5.0, 1.0)
Min droplet dia.	Minimum droplet dia. of binder droplet leaving nozzle (mm)	$(5.76\times10^{-3}, 1.15\times10^{-3})$, truncated at 7.67×10^{-3}
Max droplet dia.	Maximum droplet dia. of binder droplet leaving nozzle (mm)	$(1.92\times10^{-2}, 3.84\times10^{-3})$
Dew (i), i = 1.3	Dew point of entering fluidization air (°C) for time $T(i)$	(5.0, 1.0); (5.0, 1.0); (5.0, 1.0)
Bowl charge	Mass of powder added to batch granulater (kg)	(30.0, 6.0)
Binder (i) = 1, 3	Binder flow rate for time $T1(i)$(g/min)	(310, 62); (270,54); (250, 50)
Bed pressure (σ)	Standard deviation of pressure drop across fluid bed over experimental trial (measured) (dynes · cm^{-2})	$(1.43\times10^3, 2.80\times10^2)$
Bed pressure	Average pressure drop across fluid bed (measured) (dynes · cm^{-2})	$(1.12\times10^4, 2.24\times10^3)$
Bed length (cm)	Length of granulater (cm)	(1,500, 300)
Bed dia. (cm)	Diameter of granulater (cm) where fluidization occurs	(150, 30)
Atom − temp (°C)	Temperature of air used to atomize binder solution	(25, 5.0)
Atom − dew (°C)	Dew point of air used to atomize binder solution	(10, 2.0)
Atom − air	Air flow rate used to atomize binder solution(g cm^{-3})	$(8.0\times10^5, 1.6\times10^5)$

tion and sensitivity analysis questions, since model prediction of experimental observations is quite good. Overall, this hybrid model does an outstanding job of describing the experimental behavior over all agglomeration regimes, including regimes having multiple regions of noninertial growth (that is, more than one region of rapid agglomeration/growth). Thus, the Hybrid model can be used to predict agglomeration growth, given only process parameters for the herbicide used in the experimental trials (Flumetsulam).

The DPB model can contain up to 33 input process parameters. Thus, a model sensitivity analysis is explored to determine which input parameter(s) creates the largest variance in model output. The DPB model can therefore be used to increase understanding of sensitive process parameters beyond what is available from the experimental DOE alone.

The DPB model was written in Fortran and was altered into a stochastic−deterministic model using Monte Carlo sampling techniques through additional programming and the use of the third-party Microsoft Excel add-on Crystal Ball (Trademark of Decisioneering, Inc.). Crystal Ball allows every cell in MS Excel to be assigned a probability density function. Model input parameters were assigned a unique cell location in an Excel Worksheet, and each model input parameter was assigned a probability density function that spanned characteristic ranges associated with that variable. Visual basic for applications (VBA) programming was used with Crystal Ball libraries such that Monte Carlo techniques would sample the user-defined model input parameters, DPB model input files would be generated, the DPB model executed, and results stored back into an MS Excel worksheet. This process was repeated for 500 iterations, such that 500 unique parameter combinations were sampled and simulated. Input parameter variability for each stochastic model parameter was typically assigned a normal distribution, where the mean is given by the typical parameter magnitude (measured property), and the standard deviation was assumed to be 20% of the mean value. Several inputs were assigned a uniform distribution. Table 6 summarizes the variables and assigned PDFs used in the Monte Carlo sample of the DPB hybrid model.

Results for the DPB model sensitivity analysis are given in Figure 6 for several time intervals. Early, mid, and late intervals correspond to times within the fluid bed at approximately 18, 42, and 110 min following the start of the experiment, respectively. The nomenclature for these parameters is

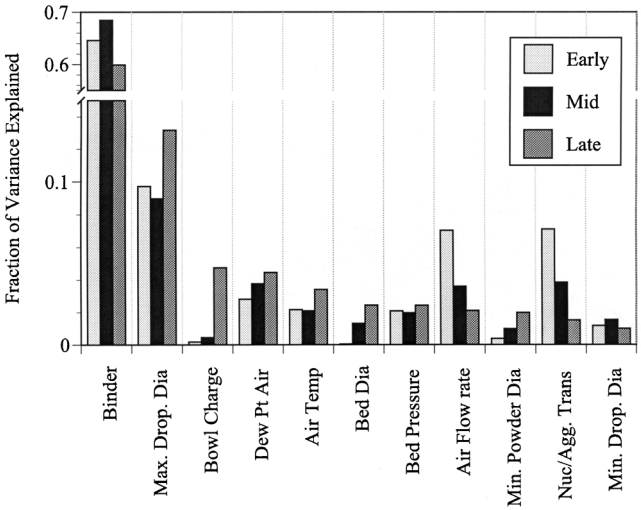

Figure 6. Model sensitivity analysis results for agglomeration processes in fluid beds.

Table 7. Nomenclature for Sensitive Process Input Parameters Summarized in Figure 6

Nomenclature	Parameter Description
Binder	Binder Spray rate
Max drop dia.	Maximum drop dia. for binder spray leaving nozzle in fluid bed
Bowl charge	Mass of powder initially placed into fluid bed (batch)
Dew pt air	Dew-point temperaature of entering fluidizing air
Air temp	Temperature of entering fluidizing air
Bed dia.	Diameter of the fluid-bed granulater
Bed pressure	Pressure drop across the bed
Air flow rate	Volumetric air flow rate of fluidizing air
Min powder dia.	Minimum dia. of starting powder
Nuc/agg trans	Transition between nucleation and agglomeration as measured by amount of binder added to the fluid bed
Min drop dia.	Minimum drop dia. for binder spray leaving nozzle in fluid bed

found in Table 7. The most sensitive parameters are represented as a fraction of explained variance for the endpoint prediction (VMD). This is based upon computing rank correlation coefficients between every parameter and the VMD, and normalizing the square of the rank correlation (such that the sum of the squared coefficients for all inputs and VMD equal one). The binder spray rate is by far the most sensitive model input, accounting for approximately 65% of the VMD variance. This is consistent with the DOE ANOVA results, only now the relative important in terms of explainable variance is quantified.

Binder addition is sensitive throughout the agglomeration process. The second most sensitive input parameter is the maximum drop diameter for the binder solution leaving the nozzle and entering the fluid bed. Maximum and minimum drop diameters for the binder spray solution were not parameters in the DOE, but are input parameters in the mechanistic DPB model. Thus, selection of different nozzles may prove advantageous when attempting to control VMD. Other slightly sensitive parameters are given in Figure 6, along with their relative contribution to the variance. These less sensitive parameters change in order of sensitivity as the agglomeration process proceeds from early to late times.

The DPB model sensitivity analysis suggests that extreme care must be exercised to reduce the variability in binder spray rate if reproducible fluid-bed trials are sought. Thus, once an optimal binder addition rate is known, proper control measures should be taken to minimize any deviations from this optimal rate to minimize variance in VMD. The binder flow rate and the size of the binder droplets entering the fluid bed drive the agglomeration process, as predicted by the numerical DPB model.

Summary

The results from the DOE presented here are consistent with expectations when explained in the context of inertia to viscous dissipation (that is, Stokes number) for particle coalescence and rebound. Four of the five primary variables (fluidizing air temperature and flow rate, binder spray rate, bowl charge), and five of ten possible two-way interactions were found to be statistically significant. Experimental observations for agglomeration growth were used with a mechanistically based DPB model to determine coalescence kernel magnitudes and to explore correlations between kernel coefficients and fluid-bed parameters. These correlations were input into the mechanistic DPB model proposed by Cryer (1999) for fluid-bed agglomeration modeling to increase understanding of the physical principles responsible for agglomeration when multiple competing mechanisms occur simultaneously.

Current simulations using the hybrid Cryer model suggest that pilot-plant fluid-bed observations can be adequately simulated in terms of predicting particle sizes of interest to the agrochemical industry, since good agreement with experiment and experimental trends is found. The model can be used for scaleup under a variety of different operating regimes and/or equipment geometries once coalescence kernel coefficient dependence on process variables is known. A mechanistic model fosters an environment for process scaleup through elimination of specific equipment and process variable constraints by focusing on the underlying mechanisms involved for proper scaleup procedures. A model sensitivity analysis obtained via Monte Carlo sampling and running the model for 500 iterations showed that the binder spray rate is the most sensitive input parameter, accounting for approximately 65% of the variance in VMD. Binder spray rate is followed by the binder droplet size leaving the nozzle and entering the fluid bed ($\sim 10\%$ of explained variance). The other three parameters found to be sensitive in the DOE (bowl charge, air temperature, and air flow rate) had explainable variances of $\sim 4\%$ each. Thus, for reproducible experimental and/or manufacturing runs, the binder spray rate should be properly controlled and kept consistent from run to run. The geometry of the fluid-bed equipment was much less sensitive than the binder inputs.

Acknowledgments

The authors thank Ron Cassel and Marty Login for operation of the fluid bed.

Literature Cited

Adetayo, A. A., and B. J. Ennis, "Unifying Approach to Modeling Granule Coalescence Mechanisms," *AIChE J.*, **43** (4), 927 (1997).

Aulton, M., and M. Banks, "The Factors Affecting Fluidised Bed Granulation," *Manufacturing Chemist and Aerosol News*, **54** (1978).

Cryer, S. A., "Modeling Agglomeration Processes in Fluid Bed Granulation," *AIChE J.*, **45** (10), 2069 (1999).

Ennis, B. J., J. Li, G. I. Tardos, and R. Pfeffer, "Strength of a Axially-Strainned Pendular Liquid Bridge," *Chem. Eng. Sci.*, **45**, 144 (1990).

Ennis, B. J., G. T. Tardos, and R. Pfeller, "A Microlevel-Based Characterization of Granulation Phenomena," *Powder Technol.*, **65** 257 (1991).

Himmelblau, D. M., *Applied NonLinear Programming,* McGraw-Hill, New York (1972).

Kao, C.-C., C.-S. Tsai, S.-C. Chen, and M.-T. Sheu, "The Application for Factorial Design to Evaluate Granular Formulation in a Fluidized-Bed Granulater," *Chin. Pharm. J.*, **48**, 355 (1996).

Olsen, K. W., "Recent Advances in Fluid Bed Agglomerating and Coating Technology," *Plant/Oper. Prog.*, **4** (3), 135 (1985).

Tatang, M. A., "Direct Incorporation of Uncertainty in Chemical and Environmental Engineering Systems," PhD Thesis, MIT, Cambridge, MA (1995).

Manuscript received Mar. 17, 2003, and revision received Apr. 14, 2003.